Intrinsic n-Type Behavior in Transparent Conducting Oxides: A Comparative Hybrid-Functional Study of In_2O_3, SnO_2, and ZnO

Péter Ágoston* and Karsten Albe

Institut für Materialwissenschaft, Technische Universität Darmstadt, Petersenstraße 32, D-64287 Darmstadt, Germany

Risto M. Nieminen and Martti J. Puska

Department of Applied Physics, Helsinki University of Technology, FIN-02015 TKK, Finland

(Received 14 September 2009; published 11 December 2009)

We present a comparative study of oxygen vacancies in In_2O_3, SnO_2, and ZnO based on the hybrid-functional method within the density-functional theory (DFT). For In_2O_3 and SnO_2, our results provide strong evidence of shallow donor states at oxygen vacancies. In comparison with the (semi)local exchange-correlation approximations in DFT, the hybrid-functional method strongly lowers the formation energy of the positive charge state and keeps that of the neutral state nearly intact. The trend is analyzed in terms of changes in lattice relaxation energies and in electron energy levels near the band gap. The existence of shallow donor states at oxygen vacancies and the consequent n-type conductivity are in line with experimental findings. The results invalidate some former theoretical interpretations based on standard DFT calculations.

DOI: 10.1103/PhysRevLett.103.245501 PACS numbers: 61.72.Bb, 61.72.jd, 71.15.Nc, 76.30.Mi

Transparent conducting oxides (TCO) are a special class of materials combining electrical conductivity with transparency for visible light [1]. Prototype TCO materials are In_2O_3, SnO_2, and ZnO. They play a key role in optoelectronic applications such as photovoltaics and are especially important as transparent electrodes used in conjunction with organic semiconductors in flat panel displays and so-called ''smart windows.''

Common features of these TCO materials are (i) intrinsic n-type conductivity accompanied with oxygen deficiency at reducing conditions, (ii) extraordinary n-type dopability, and (iii) absence of p-type conductivity. In principle, both oxygen vacancies and cation interstitials may be intrinsic donor defects [1]. However, experiments point to the formation of vacancies. Namely, the power-law dependence $\sigma_{\mathrm{el}} \sim p_{\mathrm{O}_2}^{-1/6}$ of the electric conductivity on the oxygen partial pressure, which is characteristic for doubly positive oxygen vacancies (V_{O}^{2+}), has been observed for all of these materials [2–4].

Thus far, the understanding of experimental findings for these three materials has been insufficient on the basis of electronic-structure calculations. The calculations have mainly been based on the local-density (LDA) or generalized-gradient approximations (GGA) within the density-functional theory (DFT), often including the on-site Coulomb interaction parameter U. For example, the formation energies calculated by the LDA/GGA + U method for cation interstitials are rather high, higher than those for vacancies [5–7]. On the other hand, oxygen vacancies appear as deep color centers so that no intrinsic defects have been predicted to thermally provide the free electrons observed. Moreover, formation energies predicted for acceptor defects tend to be low [5,8–10] favoring their appearance, in contrast to experiments. Explanations alternative to intrinsic donor defects have also been suggested. They involve either a persistent photo-induced process [5] for ZnO and In_2O_3 or the incorporation of hydrogen into the host material [11]. The starting assumption of these models is the validity of total energy differences in the LDA/GGA calculations.

To resolve the present experiment-theory controversy, it seems natural to probe the validity of the (semi)local DFT methods used for calculating defect properties in TCOs. The failure of the LDA/GGA is primarily manifested as too small energy band gaps in comparison with experiments. Corrections are required in order to determine the positions of the defect charge transition levels with respect to the band edges; the formation energies also have to be modified accordingly. The usual correction is to rigidly shift the band edges and/or the defect state itself. A close inspection of the magnitude of such corrections reveals that they are quite dramatic; the GGA band-gap errors are ~1.8 eV (64%), ~3.0 eV (83%), and ~2.7 eV (79%) for In_2O_3, SnO_2, and ZnO, respectively. Until now, the LDA + U method [12,13] has often been applied in defect calculations to remedy errors related to the local treatment of the exchange energy [6,14]. The method artificially shifts some semicore states, e.g., in the case of TCOs the uppermost cation d states. The effect on the band gap is indirect and partial; to correct the defect positions with respect to the experimental band gap, an extrapolation procedure is needed.

A promising alternative approach is the replacement of LDA/GGA functionals by hybrid functionals [15,16]. By including part of the exchange energy in a nonlocal manner in self-consistent calculations, they remedy the band gaps close to the experimental values. In this Letter, we present a comparative study on the role of oxygen vacancies in

In_2O_3, SnO_2, and ZnO using hybrid functionals. In contrast to LDA/GGA($+U$) functional calculations, the close agreement between the experimental and hybrid-functional band gaps does not call for further correction schemes resulting in a direct comparison of calculated vacancy formation energies and charge transition levels with the experimental ones. Our results confirm the experimental conclusions about the importance of oxygen vacancies as intrinsic donor defects. Moreover, in the following we carefully analyze the differences between the hybrid-functional and LDA/GGA($+U$) results.

The formation energy for the oxygen vacancy in charge state q reads [17]

$$\Delta G_D^q = G_{\text{def}}^q - G_{\text{host}} - \mu_O + q(E_{\text{VBM}} + E_F), \quad (1)$$

where the Gibbs free energies of the supercells with (G_{def}^q) and without (G_{host}) the defect are taken at the zero-temperature and zero-pressure limits. E_{VBM} and E_F are the positions of the valence band maximum (VBM) and the electron chemical potential, respectively. We show the formation energies only at the experimentally relevant metal rich limit where μ_O is calculated using the respective functionals. The chemical potential value of the charge transition level (q/q') is solved from the equation $\Delta G_D^q(E_F) = \Delta G_D^{q'}(E_F)$.

We use the hybrid PBE0 [18] and HSE06 [15,19] functionals as implemented in the plane-wave code VASP [20,21].

For comparison, we also employ the LDA [22] and GGA [23] functionals, as well as the GGA/LDA + U [24] method. The U values are taken from Refs. [6,7,25] for ZnO, SnO_2, and In_2O_3, respectively. The potentials due to nuclei and core electrons are presented within the projector-augmented-wave (PAW) scheme [26,27]. The d-semi-core states are treated as valence states for Zn but frozen into the core for Sn and In with the exception of test calculations with the In/Sn-4d states in the valence.

In the defect calculations, we use supercells of 72, 72, and 80 atom sites for ZnO, SnO_2, and In_2O_3, respectively. The Brillouin zone is sampled with the $2 \times 2 \times 2$ or denser equidistant k-point grids. However, the Γ-point sampling is used for the nonlocal-exchange part in PBE0/HSE06 calculations. The plane-wave cutoff energy is set to 500 eV and the forces on ions relaxed to less than 0.01 eV/Å.

We use HSE06 for In_2O_3 and PBE0 for ZnO and SnO_2, since these special choices for electronic screening are well established, tested, and allow comparison with other studies. With this choice, our hybrid-functional calculations reproduce well the experimental structure parameters ($\Delta_{\text{max}} \leq 1\%$) and band gaps (see Fig. 1).

In order to estimate the magnitude of the finite-cell-size effects in defect calculations, we have employed, within the LDA, supercells of up to 640 atom sites and extrapolated the formation energies to the infinite cell size by fitting the coefficients of the two first terms of the Makov-Payne correction [28]. Based on these calculations, we conclude that the qualitative results do not change by finite-cell-size corrections.

The formation energies of oxygen vacancies in all three TCO materials are calculated using the different functionals. The results shown in Fig. 1 reveal the existence of doubly positive (V_O^{2+}) and neutral (V_O^0) defects.

Although the formation energies reported in literature vary strongly [29], it can clearly be seen in Fig. 1 that the results obtained by using the LDA and GGA functionals are very similar. Both the formation energies as well as the charge transition levels ($0/+2$) are found at comparable values, and an n-type behavior [the level ($0/+2$) is close to the bottom of the conduction band] is only found with respect to the calculated (too small) band gap. Also, differences due to the inclusion or exclusion of the In/Sn d states in valence are always less than 0.1 eV in charge transition levels. Thus, the discrepancies in the reported values mainly result from different band-gap correction schemes used.

Applying the LDA/GGA + U method changes the results by giving slightly higher ($0/+2$) levels as well as higher formation energies for V_O^0. This is indicative for an upward shift of the defect state within the band gap. The shallow n-type behavior of In_2O_3 and SnO_2 is preserved but not that of ZnO.

For V_O^0 in different materials the hybrid functionals give essentially the same formation energies as the LDA/GGA. In contrast, the transition levels ($0/+2$) are considerably pushed upwards. This is because for V_O^{2+} the formation en-

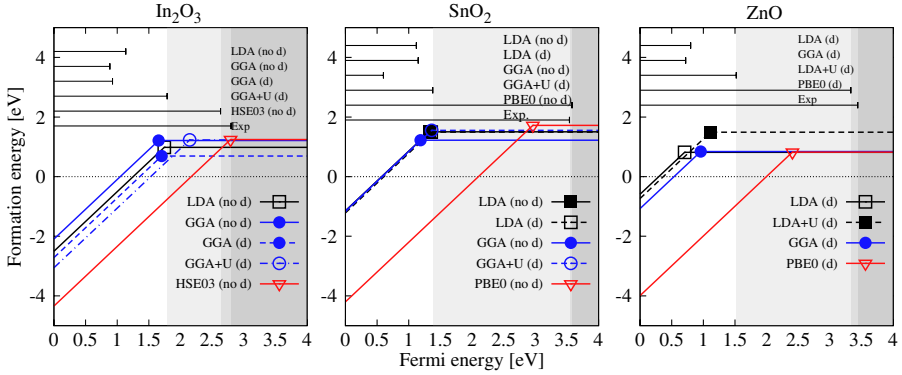

FIG. 1 (color online). Formation energies of oxygen vacancies in In_2O_3, SnO_2, and ZnO (from left to right) at reducing conditions. The lines with positive and zero slopes refer to V_O^{2+} and V_O^0, respectively. V_O^+ is unstable for all materials. The horizontal bars on the top show the calculated and experimental band gaps. The LDA/GGA + U, HSE06/PBE0, and experimental band gaps are denoted by shaded areas.

ergies decrease with respect to the LDA/GGA calculations. This is a remarkable result since the previous studies assumed more robust LDA/GGA formation energies for V_O^{2+} than for V_O^0 because the latter have no occupied defect states.

In order to analyze the reasons for the trends in the formation and charge transition levels calculated with different functionals for different materials, we plot in Fig. 2 the relaxation energies for V_O^0 and V_O^{2+} as well as the single-particle defect state positions for V_O^0. The relaxation energy is defined with respect to the defect with atoms at their ideal lattice positions. Especially in In_2O_3 and SnO_2, the relaxation energies are remarkably larger for V_O^{2+} than for V_O^0. The relaxation energies increase in magnitude from the LDA/GGA values to those of LDA/GGA + U and then especially strongly to the hybrid-functional values. The self-interaction correction inherent in the LDA/GGA + U and hybrid-functional calculations increases the ionicity; when a large ion relaxation occurs in the charged defect state, the relaxation energy also increases.

The behavior of the relaxation energy explains part of the differences between the exchange-correlation functionals in Fig. 1. The self-interaction correction lowers the VBM on the absolute energy scale [30] which favors the formation of positively charged defects with a further decrease of the formation energy. These two reasons are not effective for V_O^0 and their formation energies do not vary much in Fig. 1.

The LDA/GGA(+U) gives clearly higher formation energies for V_O^{2+} than the hybrid functionals. For V_O^0, the differences are not so large. But, as seen in Fig. 2, the oxygen vacancy defect state rises for all materials when going from LDA/GGA to LDA/GGA + U; if extrapolation techniques or other band-gap corrections [6] shifting the defect state in the band gap are also applied to the LDA/GGA + U results, the neutral-state formation energies would increase strongly. This would lead to the conclusion that oxygen vacancies are not abundant in thermal equilibrium in n-type oxides.

Our results show that the band offset for a scissorlike band-gap correction should mainly be attributed to the VB in contrast to previous studies. More importantly, we show that the relaxation energies predicted by the LDA/GGA are by more than 0.5 eV smaller than those calculated by hybrid functionals. This is an energy contribution which cannot be covered by band-edge shifting at all. The combined effect of errors in relaxation energies and in band-gap correction can lead to qualitatively wrong predictions.

The proper solution of the band-gap problem is critical in the case of In_2O_3. Namely, on the basis of LDA/GGA calculations [5], the oxygen vacancy is conjectured to form a color center in In_2O_3, whereas in our hybrid-functional calculations the vacancy is turned into a shallow donor with a low formation energy. Thus, our results explain the observed n-type behavior and oxygen deficiency.

According to our hybrid-functional calculations, the n-type behavior is favored also for SnO_2 although the

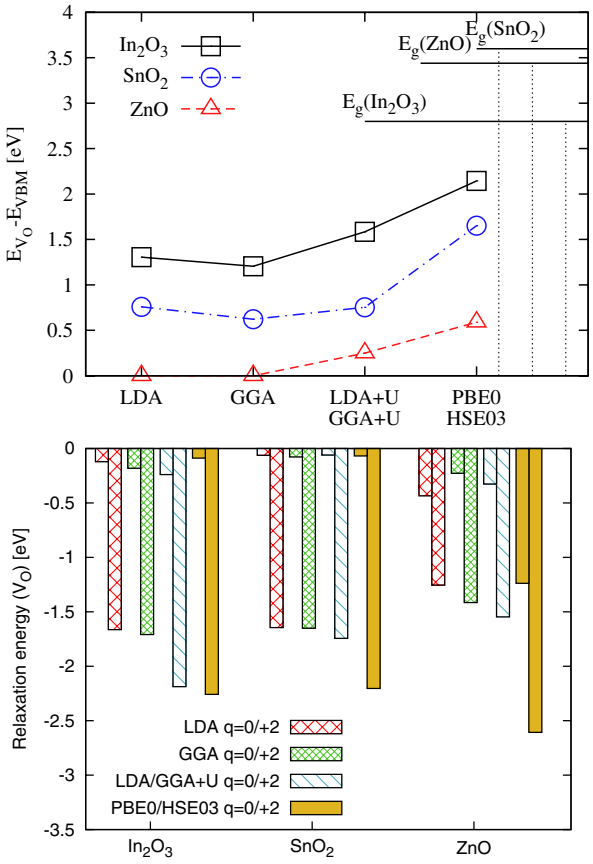

FIG. 2 (color online). (Top) Distance of the V_O^0 defect state from the VBM calculated with different functionals. (Bottom) Relaxation energies for oxygen vacancies in In_2O_3, SnO_2, and ZnO calculated with different functionals. In each case, the left and right bars denote V_O^0 and V_O^{2+}, respectively.

oxygen vacancy state remains rather deep, around 0.5 eV below the conduction band minimum (CBM). This trend is in accord with experiments which indicate that intrinsic electron concentrations are usually lower for SnO_2 than In_2O_3 samples [1]. Moreover, the $p_{O_2}^{-1/6}$ dependence of double-charged donors has been observed in SnO_2 only at rather high temperatures, which makes donor states shallower through entropic contributions and a pronounced band-gap narrowing [31]. Also, in the case of SnO_2, our results are in sharp contrast to previous calculations [7,10], which predict deep donor defects more than 1.8 eV below the CBM. We stress that beside the $\sigma \sim p_{O_2}^{-1/6}$ dependence indicating the presence of oxygen vacancies, a hydrogen-induced increase of the n-type behavior has also been observed experimentally [3]. Hence we suggest that both defects contribute to the thermal electron donation depending on the environment and temperature.

We find that in ZnO the oxygen vacancy is a color center. This is in agreement with previous hybrid-functional studies [8]. In comparison with the LDA results [6], the transition level (0/ + 2) is shifted towards the CBM by ~1.5 eV because the formation energy of V_O^{2+} decreases by more than 3 eV. The formation energy of the oxygen

vacancy is low, less than 1 eV, which naturally explains the nonstoichiometry. However, only an insufficient fraction of the electrons will become excited at ambient temperatures in order to explain the high electrical conductivity observed. Therefore, it seems plausible to assume that also other mechanisms may contribute to the electrical conductivity depending on the external conditions. According to experiments, the photoconductivity decay time is long in ZnO [32] which makes a high average fraction of ionized vacancies [5] possible. This explanation is also supported by the present study which predicts that a large ionic relaxation occurs when V_O^{2+} traps electrons.

Our results have a general implication for all of the studied TCO materials regarding the possibility of *p*-type doping. Namely, the low formation energies predicted by hybrid-functional calculations are so low that for the oxygen-rich growing conditions the oxygen vacancy formation energies also become even negative for the electron chemical potential near the VBM. This indicates that *p*-type doping is impossible for these materials close to the thermodynamic equilibrium.

Finally, we analyze the impact of the semicore *d* states on the valence band structure of In_2O_3 and SnO_2. The LDA/GGA + *U* correction opens their band gaps by affecting on the *d*-state positions. Our hybrid-functional calculations produce band gaps in a reasonable agreement with experiments for both materials; i.e., they are ~3.6 eV and ~2.6 eV for SnO_2 and In_2O_3, respectively. Further, in comparison with the LDA/GGA results, the semicore states shift downwards due to the reduced self-interaction errors. However, according to our hybrid-functional calculations, the band gap is not sensitive to the inclusion of the *d* states in valence by more than 0.02 and 0.2 eV for SnO_2 and In_2O_3, respectively. We therefore conclude that the self-interaction of *d* states cannot be a major reason for the band-gap error and suggest that the LDA/GGA + *U* method applied on *d* states is not a physically motivated approach to remedy the band-gap problem.

In summary, we conducted a comparative study on the intrinsic *n*-type conductivity of three TCO base materials In_2O_3, SnO_2, and ZnO. We applied the advanced hybrid-functional methodology beside the extensively used (semi) local DFT methodology. We identified major weaknesses of the standard LDA/GGA and tested conventional band-gap correction schemes in comparison with the hybrid PBE0/HSE06 functionals. We found that rigid shift corrections are not able to reproduce the hybrid-functional results. This is partly because the LDA/GGA severely underestimates (by more than 0.5 eV) the relaxation energies in vacancies. This underestimation cannot be covered by band-edge shifting. According to our hybrid-functional calculations, the oxygen vacancy is in In_2O_3 and SnO_2 at reducing conditions a shallow donor with a low formation energy. This strongly supports the viewpoint arising from experiments that abundant oxygen vacancies are the cause of the intrinsic *n*-type behavior. For ZnO, our results hint for a more complex donation mechanism.

We acknowledge financial support through the SFB 595 of the DFG, DAAD and the Academy of Finland through its Center of Excellence Program (2006–11). Discussions with Ari P. Seitsonen are acknowledged. This work was made possible by grants for computing time at CSC computing facilities in Espoo, Finland and HHLR Darmstadt as well as FZ Jülich.

*agoston@mm.tu-darmstadt.de

[1] H. L. Hartnagel, A. K. J. Dawar, and C. Jagadish, *Semiconducting Transparent Thin Films* (Institute of Physics Publishing, Bristol, 1995).
[2] G. Rupprecht, Z. Phys. **139**, 504 (1954).
[3] S. Samson and C. G. Fonstad, J. Appl. Phys. **44**, 4618 (1973).
[4] K. I. Hagemark, J. Solid State Chem. **16**, 293 (1976).
[5] S. Lany and A. Zunger, Phys. Rev. Lett. **98**, 045501 (2007).
[6] A. Janotti and C. G. Van de Walle, Phys. Rev. B **76**, 165202 (2007).
[7] A. K. Singh *et al.*, Phys. Rev. Lett. **101**, 055502 (2008).
[8] F. Oba *et al.*, Phys. Rev. B **77**, 245202 (2008).
[9] P. Ágoston and K. Albe, Phys. Chem. Chem. Phys. **11**, 3226 (2009).
[10] C. Kilic and A. Zunger, Phys. Rev. Lett. **88**, 095501 (2002).
[11] C. G. Van de Walle, Phys. Rev. Lett. **85**, 1012 (2000).
[12] V. Anisimov *et al.*, Phys. Rev. B **48**, 16929 (1993).
[13] A. Liechtenstein *et al.*, Phys. Rev. B **52**, R5467 (1995).
[14] S. Lany and A. Zunger, Phys. Rev. B **78**, 235104 (2008).
[15] J. Heyd, G. E. Scuseria, and M. Ernzerhof, J. Chem. Phys. **118**, 8207 (2003).
[16] J. Paier *et al.*, J. Chem. Phys. **124**, 154709 (2006).
[17] S. B. Zhang and J. E. Northrup, Phys. Rev. Lett. **67**, 2339 (1991).
[18] J. Perdew, M. Ernzerhof, and K. Burke, J. Chem. Phys. **105**, 9982 (1996).
[19] J. Heyd, G. E. Scuseria, and M. Ernzerhof, J. Chem. Phys. **124**, 219906 (2006).
[20] G. Kresse and J. Furthmüller, Phys. Rev. B **54**, 11 169 (1996).
[21] G. Kresse and J. Furthmüller, Comput. Mater. Sci. **6**, 15 (1996).
[22] D. M. Ceperley and B. J. Alder, Phys. Rev. Lett. **45**, 566 (1980).
[23] J. P. Perdew, K. Burke, and M. Ernzerhof, Phys. Rev. Lett. **77**, 3865 (1996); **78**, 1396(E) (1997).
[24] S. L. Dudarev *et al.*, Phys. Rev. B **57**, 1505 (1998).
[25] P. Erhart, A. Klein, R. G. Egdell, and K. Albe, Phys. Rev. B **75**, 153205 (2007).
[26] P. E. Blöchl, Phys. Rev. B **50**, 17 953 (1994).
[27] G. Kresse and D. Joubert, Phys. Rev. B **59**, 1758 (1999).
[28] G. Makov and M. C. Payne, Phys. Rev. B **51**, 4014 (1995).
[29] S. Lany and A. Zunger, Phys. Rev. B **78**, 235104 (2008).
[30] A. Alkauskas, P. Broqvist, and A. Pasquarello, Phys. Rev. Lett. **101**, 046405 (2008).
[31] E. Kohnke, J. Phys. Chem. Solids **23**, 1557 (1962).
[32] R. Laiho *et al.*, J. Appl. Phys. **106**, 013712 (2009).